Technical Report

UDC 621 . 791 . 763 . 3 : 669 . 14 - 462 . 2

Development of a New Optical Monitoring System for HF-ERW Welding Processes

Noboru HASEGAWA*
Toshisuke FUKAMI
Yusuke TAKEDA
Michitoshi TANIMOTO
Hideki HAMATANI
Tomohiro NAKAJI
Takashi MOTOYOSHI
Takashi OHSAWA

Abstract

To satisfy recent demands for high mechanical strength and toughness in the weld seam for the pipeline fields, we propose a manufacturing technique that controls the generation of cold defects and oxide inclusion in the welding process. By analyzing the welding mechanism, we optimize the welding condition and develop a new monitoring system that combines optical and electrical measurements. We demonstrate that the system improves the weld seam quality of high frequency-electric resistance welded (HF-ERW) pipe in our 24" product process of Hikari works.

1. Introduction

In recent years, in accordance with the demand for the exploitation of energy in its background, demand for application of low-cost, efficiently producible electric resistance welding (ERW) pipes to line pipe and oil well market is growing. For this application, improvement of the material characteristics and resistance to environment not only of the parent material but also of the welded part is required. For such a purpose, production technologies become necessary that suppress the occurrence of defects, such as cold-weld, owing to insufficient power input during welding to welded part and defects attributed to the formation of oxides in the welded part. To date, authors have tackled the development of a weld monitoring system as a part of quality enhancing project activity to control and maintain welding conditions at an optimum level based on welding mechanism. This article reports the result of the introduction of a heat-input-control method based on an optical and electrical measuring system developed through the analysis of the relationship between welding phenomena and weld quality.

2. About ERW

It is a process of forming a steel sheet into a circular shape, inducing high-frequency current by applying high-frequency voltage to weld surface through a work coil or electrodes called as contact tip, locally heating, and welding. In this welding process, since most of the current is concentrated near the vicinity of the weld surface by skin effect and proximity effect, efficient heating of abutting surfaces is possible (**Fig. 1**). Furthermore, an oxide film is formed on the weld surface in the heating process; however, the oxide is discharged together with molten steel by the currents that flow counter to each other on both edge surfaces, and the discharging is further promoted characteristically in the upsetting process by squeeze rolls. This welding is a production method that was introduced to the actual process in the earlier half of the 1900s. However, in the

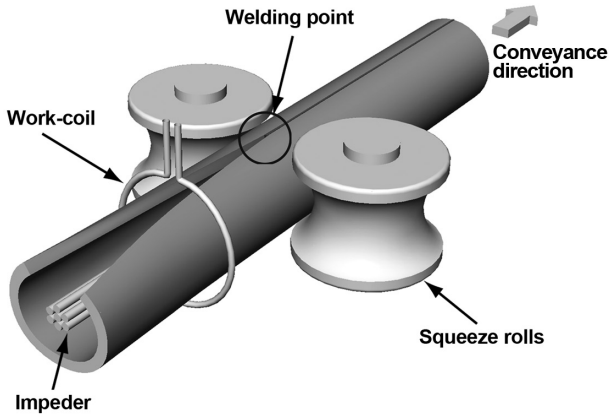

Fig. 1 Outline of the HF-ERW

* Senior Researcher, Ph.D., Instrument System R&D Div., Process Research Laboratories
20-1 Shintomi, Futtsu City, Chiba Pref. 293-8511

old low-frequency welding, there existed a so called Zipper weld problem, where unwelded welds came into existence when the current became zero. To overcome this problem, high frequency of several hundred kHz high frequency-ERW was applied, which resulted in drastic improvement of the weld quality.

3. Development for High Quality of Welded Part

3.1 Understanding the welding phenomena

3.1.1 Concept of welding process

ERW welding is a complicated process in which the welding condition is influenced by various factors such as pipe diameter, wall thickness, input power, welding speed, convergence state of both edges, angle of weld surface, and distance between the power supply point and edge contacting point. Since some of these factors are hard to control independently, the method of approach has been to grasp the emergence of welding phenomena relevant to particular factors. So far, the condition phenomena defect (CPD) diagram, an interrelation diagram focusing on the relation between input power and welding speed, has been proposed. **Figure 2** shows a schematic figure when factors other than welding speed and input power are assumed to remain unchanged. Major boundaries are indicated by the Line A, which shows the line where the rate of approach and that of retreat of both edges of the steel material become equal, and the Line B, which shows the melting limit of the entire edge surfaces. In the spheres formed by the boundary lines, the welding phenomena termed as Types 1, 2, and 3 emerge, each respectively corresponding to the cold-weld or unwelded-weld-causing condition, the optimum condition, and the excessive power input condition. Among them, stable welding phenomena are considered to emerge in Type 2 when power above the Line A is input at the welding speed higher than the critical welding speed of Vm where the Lines A and B intersect.[1-3)]

The welding process involves three processes: heating, melting, and discharging. In the heating process, the temperature starts to rise at the edge part at application of a high-frequency voltage, and in accordance with this, formation of oxide films on the surfaces is promoted. In an ideal state in the melting process where sufficient power is input, the molten portion of the steel is soon made to flow toward the upper and lower side surfaces of the abutting surfaces by the electromagnetic force produced by the high-frequency current. At the final discharging process, when upsetting is applied properly by the squeeze rolls, metal flows become vertical and the residual oxides is discharged from the abutting surfaces together with the molten steel. When, at this moment, there is no sufficient input power (low power input below the Line B), melting on both edge surfaces is insufficient and edges are not welded (state of cold-weld or unwelded welding) even if the upsetting is applied. On the other hand, in Type 3 where power input is excessive, a slit grows extremely long, and if a short circuit takes place in the upstream side of the slit under this condition, the electromagnetic force in the downstream side disappears, and this disappearance causes a phenomenon of reflow of molten steel into the slit. Furthermore, since upsetting does not function sufficiently, oxides are not discharged properly and penetrator defects attributed to the residual oxides grow. Up to the present, it has been considered that, in the Type 2 sphere, heating–discharging is performed properly; therefore, a high-quality-welded-part with few defects can be obtained. However, as a result of an experiment and a model analysis, it has been found that there is a possibility that the Type 2 sphere can be divided into three spheres from the viewpoint of weld quality.

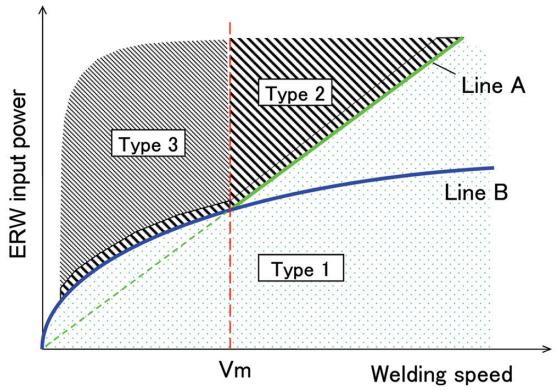

Fig. 2 CPD diagram

3.1.2 Analysis of welding phenomena in Type 2

To clarify the relationship between input power and weld defects, an experiment using an off-line welding machine that enables welding of a narrow-width steel strip under varied conditions was carried out and the fractured section surfaces were examined. Welding was conducted in the following conditions: sheet thickness: 6 mm, sheet width: 32 mm, material: API Standard X65, amount of squeezing (stroke of pressurizing): 4 mm, Vee convergence angle: 5.0°, welding speed: 32 m/min of above the critical welding speed of Vm. A Charpy impact test at 160°C was carried out for the welded part of several samples processed with power input varied in the range 390–830 kVA, and the area of the defects on the fractured surface was assessed with a stereoscopic microscope. The fractured surface obtained at this temperature exhibits ductile fracture in the normal part, while on the other hand, exhibits brittle fracture in the defective part and cold-weld part, therefore, identification of normal/abnormal parts is possible.

Figure 3 shows an example of dependency of the defect area ratio on power input obtained by this assessment. In the Type 2 sphere where the power input is above 460 kVA, the defect ratio is low; however, in some cases, a sphere between 550 and 620 kVA emerges, which shows a relatively high defect ratio, and therefore it is found that there are three spheres in terms of weld quality. These three spheres are termed as Type 2, Transitional region, and Type 2' sphere in the order from the low power input side. Furthermore, as this curve shifts toward the higher input power side in case centeroffness in abutting of the weld surfaces in the I shape takes place. Therefore, it was considered that the Type 2' sphere is most optimized.

3.1.3 Observation of the phenomena with images[4)]

In **Fig. 4**, the welding phenomena are illustrated on the basis of the images of steel sheet edges taken by a high speed camera from above the welded part. Power is supplied to the steel via contact tips (or a work coil) while the steel is being conveyed from the left side to the right side and pressurized by the squeeze rolls the moment when both edges come into collision-contact. Here, attention should be paid to the behaviors of points, which are very important to clarify the welding phenomena; the geometric convergence point of steel material edges (Point V0), the convergence point of collision-contact of both edges (Point V1), and the welding point where upsetting is applied and started (Point W). Under the Type 1 condition, steel sheet edges form a simple V shape where all three points fuse into a single common point.

In the Type 2, where the power input is increased from the previ-

ous state, only the Point W moves toward downstream. This is because the rate of approach of the edges in conjunction with the conveying movement of the steel and that of retreat of the edges in conjunction with the outward discharging of the molten steel from the edges by electromagnetic force reach the same rate, and a narrow gap called slit grows between the two edges. In the slit, a phenomenon called "bridge travelling behavior"[5] wherein a bridge travels within the slit at the cyclic rate of several hundred Hz per second and slit expansion/contracting thus caused are observed. The entire slit length grows longer as the welding condition moves from Type 1 to Type 2, and becomes almost constant at the upper limit of the Type 2 sphere. Since it is a gap that penetrates through the sheet in thickness direction, emergence of the slit suggests the melting of the entire edge surfaces.

In the Type 2' where the heat input is further increased, Point V1 leaves Point V0 and moves toward downstream, and in the upstream side of V1 and after V0, the edges retreat in a departing manner from the original position. Furthermore, it is observed that both edges do not form a simple V letter shape, but form Vee convergence angles at two steps (convergences at two steps). This phenomenon emerges as a result of the rate of retreat of both edges being slightly higher than that of the approach, in addition to the state of the melting of the entire edge surfaces. Furthermore, even when the abutting surfaces form V shape with each other, if the difference between the gap distance at the upper surface and lower surface is smaller than that of the original, it is considered that the entire edge surfaces are molten.

Moreover, in the early stage of emergence of the two-step convergence, a phenomenon of Point V1 moving between Point V0 and Point W for a considerable length appears. This is because of the occurrence of collision-contacting of edges in the upstream of the slit due to the variation of forming, the condition of edges, and so on as the distance between the edges in the second convergence is very small. At this moment, electromagnetic force in the downstream of the collision-contact point is lost temporarily; therefore, oxides cannot be discharged properly by the electromagnetic force during melting and defects tend to increase. This power input condition is called as a transitional region.

3.2 Development of weld monitoring technology

3.2.1 Method of observation

For the verification of melting in the actual production process, an optical and electrical welding process monitoring technology has been developed with the aim of controlling the power input to be within the Type 2' sphere that accompanies the two-step convergence (**Fig. 5**).

a) Optical photographing: The red-hot pattern at the steel sheet edge is optically photographed by a color-separating color CCD camera at the rate of 40 fps. Spatial resolution of less than 100 μm is required for detecting the slit part of width of several hundred μm. Furthermore, since there is a bridge traveling behavior phenomenon

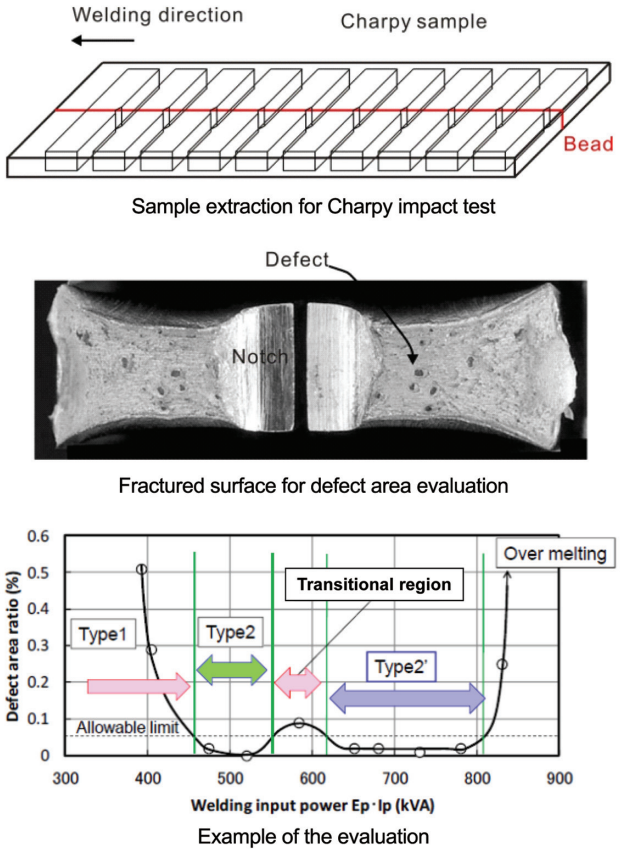

Fig. 3 Evaluation of defect ratio versus heat input powers

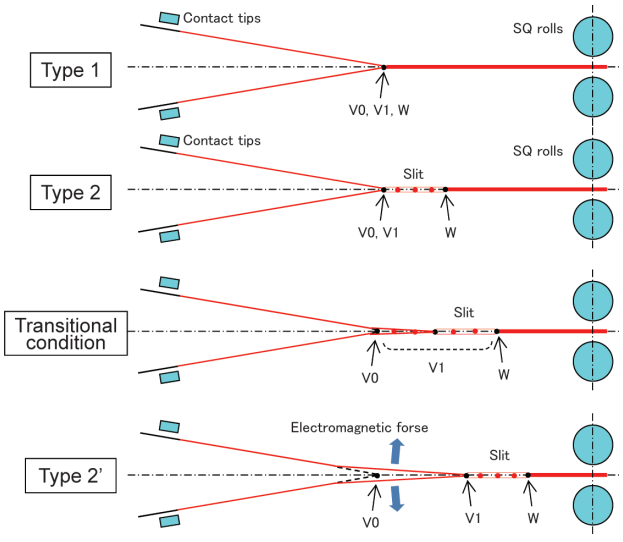

Fig. 4 Observed welding phenomena in various heat input powers

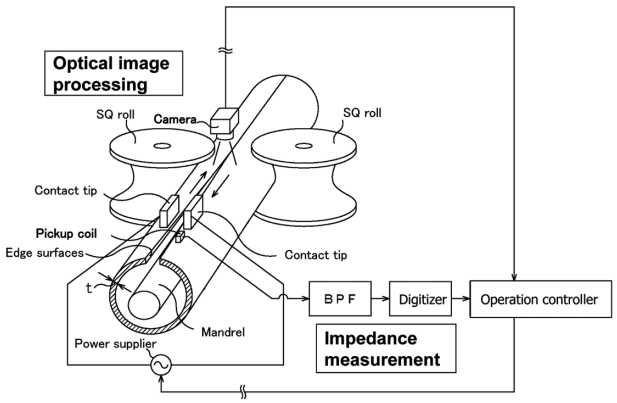

Fig. 5 Configuration of the welding observation methods

in the slit, which causes slit expansion/contraction at a high rate as mentioned earlier, photographs are taken with the exposure time of about 1/10 000 s. The photographic images taken are processed real time, and the information necessary to judge the appropriateness of power input and the normality/abnormality of the welding condition is detected continuously along the entire length.

b) Measurement of frequency of induced current: Change in the electromagnetic field produced by the high-frequency current applied to the steel is measured using a pickup coil installed adjacent to the power supplying contact tip. As the frequency component of the detected signal is proportional to the length of the current path, the amount of the change in frequency shows the change in the impedance developed by the slit expansion/contraction. With this measurement method, it is possible to determine the heat input condition based on the condition of the slit. Slit grows gradually in accordance with the transition from the Type 1 to Type 2 sphere. During this period, signal changes in short cycle when the slit length is short, on the other hand, the signal shifts toward longer cycle side as the slit grows. Accordingly, when the power input is increased gradually from the low power input side, change in frequency caused by the growth of the slit in the transition from the Type 1 to Type 2 sphere is observed.

Although the rate of measurement of the optical method is not high, the method is superior in the visual recognition of the Vee convergence, and the conditions of the respective V point are possible. However, since the measurement of the frequency has the rate of sampling above 1 MHz, it can capture very high speed phenomena. By utilizing these two methods in a mutually complementary manner, it is possible to judge the welding condition accurately and stably.

3.2.2 Verification of melting of entire edge surfaces [6)]

To investigate the welding condition that melts the entire edge surfaces, the melting was verified off-line. A thermocouple was inserted into the center position in the thickness direction of the abutting steel sheets, and photographs were taken with the aforementioned system while measuring the temperature (**Fig. 6** (a)). Figure 6 (b) and (c) show the trends in the measured temperature changes and the corresponding photographic images, respectively. It is interpreted that in the Type 1 condition, once the temperature reaches the melting point of the steel, the steel is solidified again within 10 ms.

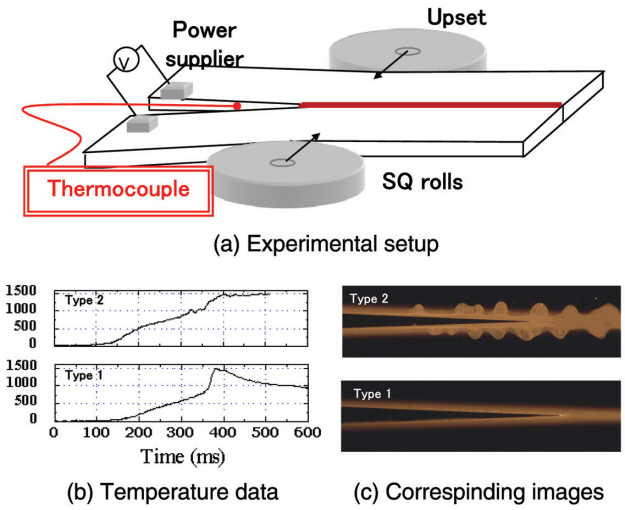

Fig. 6 Experiment for clarifying melting of the entire edge surfaces

Whereas, in the Type 2, it is presumed that the molten state of the center of the steel sheet is maintained for longer than 100 ms and the molten steel is discharged by the squeezing pressurization. In the transitional region and in the Type 2', since larger amount of heat is input, it is considered that the entire edge surfaces are molten to the center.

3.2.3 Image processing method to detect welding condition

In order to judge the welding condition in the Type 2' sphere, automatic detecting function of aforementioned points V0, V1, and W and Vee convergence angle is required (**Fig. 7** (a)). For detection in a stable manner, the following algorithm was programmed: (1) extract the red color component from the color images taken; (2) in the edge detection area that is 70% of the upstream area of the Vee convergence formed by the two edges, edge positions are sought for and determined, and approximation lines are derived with minimum square method (Fig. 7 (b)), and, simultaneously, the Vee convergence angle is sought for; (3) the angle between the two lines is determined as Vee convergence angle and the crossing point is determined as V0; (4) the image data of Vee convergence part is reversibly binary-processed and labelled, and the utmost downstream end point of the blob is determined as V1 (Fig. 7 (c)); and (5) among the blobs that exist downstream of V1 along the bisector of the convergence angle, blobs having small aspect ratios are connected and the point at the utmost downstream is determined (Fig. 7 (d)). For the slit expansion/contraction, detection positions in images of more than several frames are memorized and the point detected at the utmost downstream end is determined as Point W. In addition, a blob means a group of pixels developed by connecting four or eight picture elements, which exist adjacent to each and labelled as identical in labelling processing.

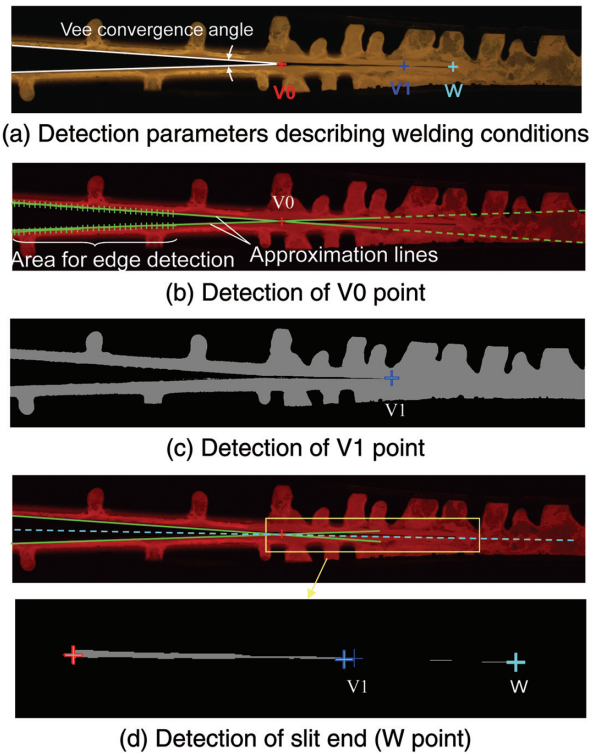

Fig. 7 Image processing algorithm

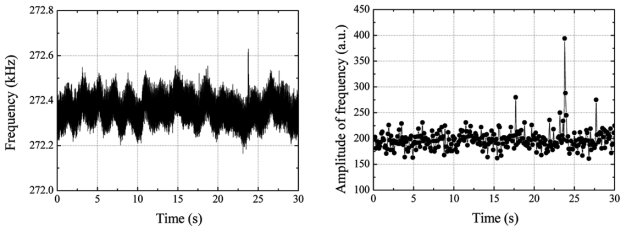

Fig. 8 Typical result of multi-frequency filtering

3.2.4 Development of digitization of induced current waveform

Measuring equipment of induced current has been applied to production process up to present; however, it was limited to showing waveform in analog form. Then, the equipment was converted to enable data processing of the measured data in a digital processing manner by newly installing an A/D converter. With this, noise cutting has been made easier by setting signal processing parameters freely, and the merit of preserving data possible for long term has also been brought forth. Here, an example is introduced where the continuous monitoring of welding condition and judgment of abnormality have been made possible by adding multi-frequency filtering function. From the measured waveform shown on **Fig. 8** (b), the amplitude of the change in the frequency of the high-frequency current can be measured and, as mentioned above, slit expansion/contraction behavior can be understood. However, this was impossible with the row waveform where the power source ripple and its higher harmonious waves were overlapped, making detection of abnormal phenomena difficult. Then, multi-frequency digital filtering processing for cutting signals in pluralities of specific frequency zone, such as of power supply source and applied voltage, was installed after the A/D converter. Thereby, detection of sparks that may cause defects (spike-like figure in Fig. 8 (b)) has been made possible.

3.3 Introduction of the system to actual production line

The monitoring system for use in an actual production line equipped with the above mentioned welding condition judging and spark-detecting functions has been introduced to the 24" mill of the Hikari Pipe and Tube Department. In this system are also incorporated the initial setting of the amount of heat input, real-time renewal of CPD diagram, monitoring of temperature of the welded part and the detecting function of weld abnormalities, and the monitoring of welding condition over the entire length.

By applying this system to the test material with wall thickness of 12.7 mm and X65 of API Standard, verification of the performance in actual operation and the establishment of numerical standards of the line operating parameters were carried out by varying the power input from the heat input standard in operation (lower limit of the Type 2 sphere) to standard +20%. **Figure 9** shows the result of the study on the relation between the power input at various levels and the corresponding defect area ratios. This data shows that Type 2 and Type 2' are the most optimum welding conditions and a region sometime exists between the two conditions where the defect ratio increases, a trend similar to that of the off-line test.

Examples of photographed images corresponding to these test conditions are shown in **Fig. 10** (a). As the power input becomes larger, Point V0 (shown in red in the figures), Point V1 (blue), and Point W (light blue) move systematically in accordance with the change in power input. It is found that at the heat input standard, all points are observed to gather on a single point; however, Point V0 moves toward upstream and Points V1 and W move toward downstream as the power input is increased, and when the power input reaches above heat input standard +15%, Point V1 departs Point V0, and a region where Vee convergence angle at two steps emerges.

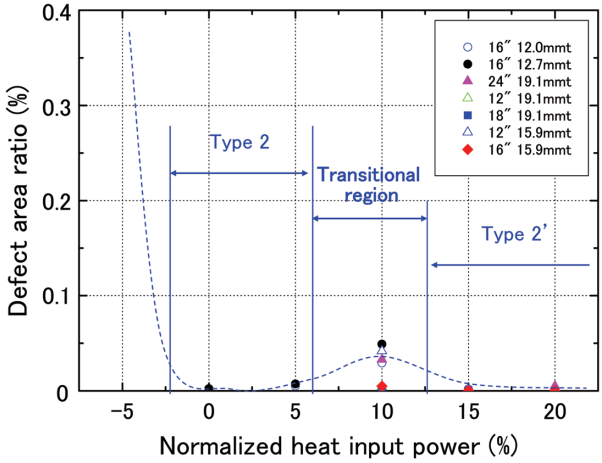

Fig. 9 Defect area ratio evaluation of X65 products

From the result of processing of photographic images taken continuously for 3 s under these heat input conditions (Fig. 10 (b)), it is found that while all points are observed to come to a single point below the condition of heat input standard+5%, in the condition of above heat input standard +15%, V0 and V1 always exist apart from each other and the state of the two-step convergence is exhibited. Since, at this moment, candidate point W moves toward downstream with a certain probability, it is judged that the slit expansion/contraction behavior can be captured at the photographing rate of 40 fps. Furthermore, under the condition of heat input standard +10% (transitional region), an unstable phenomenon is observed where Point V1 irregularly hops between Point V0 and Point W. In addition, since the conditions of heat input standard and heat input standard +5% correspond to the Type 2 sphere, there should be slits, which are not clearly recognizable on the photographic images.[6)]

Furthermore, the frequency waveform of the induced current (Fig. 10 (c)) also supports this finding. As mentioned before, the magnitude of the amplitude shows the behavior of the slit; therefore, it is understood that under the condition of heat input standard, the slit is in the process of growing, and under the condition of heat input standard +5%, relatively long slit exists. Under the condition of above heat input standard +15%, stable slit expansion/contraction is observed, on the other hand in the transitional region, it is presumed that the slit extends very long and expansion/contraction is taking place at a relatively long cycle.

In the measurement of frequency of the induced current in this way, it is not easy to know the detail of the change in heat input in the Type 2' sphere; however, the growth of the slit is observable in the vicinity of the lower limit of Type 2'. On the other hand, with optical photographing, it is possible to quantify the change in heat input under the condition of above heat input standard+15% based on the distance between V0 and V1. But it is difficult to detect the slit at the early stage of its growth. By utilizing measurement information obtained by these two methods in a mutually complementary manner, understanding in a wider range of the welding condition in the actual production process has become possible.

Based on the above data, the welding condition of the actual production process was continuously monitored and heat input was controlled to stay in the state of the two-step convergence in the

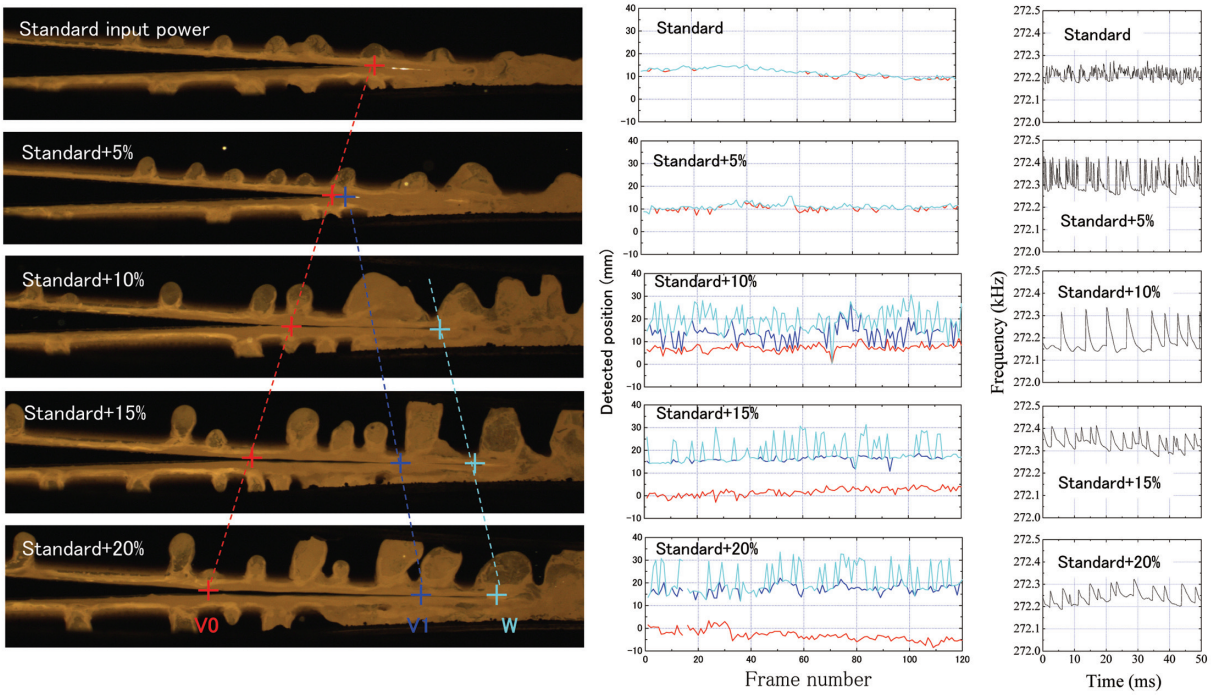

Fig. 10 Real-time monitoring of the welding phenomena in Hikari 24" process

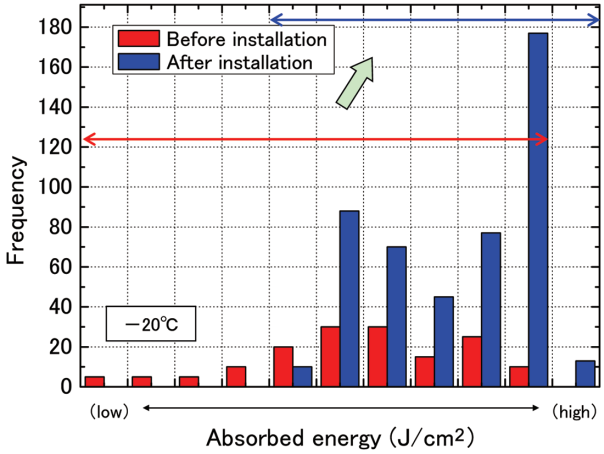

Fig. 11 Improvement of the seam quality in Hikari 24" process

Type 2' sphere. It was found that the defect area ratio of trial products of wall thickness of 9.5–19.1 mm and other commercial products was controlled on the entire length. As a result, the variation in quality could be improved (**Fig. 11**).

4. Conclusion

In ERW welding, it was found that the Type 2 welding sphere, which has been long known as the most optimum condition from the viewpoint of welding quality, is to be divided into three sub spheres including a transitional region. It was experimentally verified that among them, a two-step convergence phenomenon observed in the Type 2' sphere is the verification of the melting of the entire abutting edge surfaces. The defect ratio can be controlled mostly in the actual production process where there is a possibility of abutting angle being varied. Then, to control the welding condition to be within the Type 2' sphere, authors developed the weld monitoring technology by employing the real-time image processing and frequency measurement of induced current and applied the technology to the actual production process and confirmed that the quality of the welded part can be controlled at a high level.

References

1) Haga, H.: Weld. J. Res. Suppl. July, 208 (1980)
2) Haga, H.: Weld. J. Res. Suppl. June, 104 (1981)
3) Haga, H.: Nippon Steel Technical Report. (26), 27 (1985)
4) Fukami, T., Mizuhashi, N., Hasegawa, N., Hamatani, H., Hasegawa, Y., Asano, T., Motoyoshi, S., Miura, T., Tanaka, K., Nakaji, T., Yamamoto, K.: Proc. Int. Pipeline Conf. 90219, 2012
5) Kim, C-M., Kim, J-K.: J. Mat. Process, Technol. 209, 838 (2009)
6) Hasegawa, N., Hamatani, H., Mizuhashi, N., Fukami, T., Karube, Y., Miura, T., Tanaka, K., Nakaji, T., Yamamoto, K., Hasegawa, Y.: Proc. Int. Pipeline Conf. 90222, 2012

Noboru HASEGAWA
Senior Researcher, Ph.D.
Instrument System R&D Div.
Process Research Laboratories
20-1 Shintomi, Futtsu City, Chiba Pref. 293-8511

Hideki HAMATANI
Chief Researcher, Dr.Eng.
Nagoya R&D Lab.

Toshisuke FUKAMI
Senior Researcher
Pipe & Tube Research Lab.
Steel Research Laboratories

Tomohiro NAKAJI
Senior Manager
Plant Engineering Div.
Plant Engineering and Facility Management Center

Yusuke TAKEDA
Hikari Pipe & Tube Div.
Oita Works

Takashi MOTOYOSHI
Senior Manager, Head of Dept.
Hikari Pipe & Tube Div.
Oita Works

Michitoshi TANIMOTO
Senior Manager
Tubular Products Technology Div.
Pipe & Tube Unit

Takashi OHSAWA
Senior Manager, Head of Dept.
Tubular Products Technology Div.
Pipe & Tube Unit